

## The Drag-free CubeSat

John W. Conklin, Karthik Balakrishnan, Sasha Buchman, Robert L. Byer, Grant D. Cutler, Dan B. DeBra,  
Eric Hultgren, John A. Lipa, Shailendhar Saraf, Seiya Shimizu, Andreas Zoellner  
Stanford University  
Hansen Experimental Physics Laboratory, Stanford, CA 94305-4085; 1-650-308-6351  
johnwc@stanford.edu

Abdul Alfauwaz, Ahmad Aljadaan, Hamoud Aljibreen, Mohammed Almajed, Turki Al-Saud, Badr Alsuwaidan,  
Salman Althubiti, Haithem Altwaijry  
King Abdulaziz City for Science and Technology  
P.O Box 6086, Riyadh 11442, Saudi Arabia

Paolo Bosetti  
University of Trento  
via Mesiano 77, I-38123 Trento, Italy

### ABSTRACT

A drag-free spacecraft utilizes a Gravitational Reference Sensor (GRS) to shield an internal free-floating test mass (TM) from (a) external disturbances and (b) from disturbances caused by the spacecraft itself. The GRS measures the position of the spacecraft with respect to the TM and a feedback control system commands thrusters to maintain that position. In principle, the test mass is then completely freed from non-gravitational disturbances so that it and its “tender” spacecraft follow a pure geodesic. To date, three drag-free spacecraft have flown: TRIAD I in 1972, which provided the first navigation by satellite, Gravity Probe B in 2004, which tested predictions of Einstein’s general relativity theory, and the 2009 geodesy mission, GOCE (Steady-State Ocean Circulation Explorer). Next generation GRS technology for geodesy, fundamental physics and gravitational wave detection in space, has been under development at Stanford since 2004. Most recently a small scale instrument, called the 1U GRS has been proposed for a 3U CubeSat primarily for Earth aeronomy and geodesy applications. The 1U GRS consists of a 25 mm diameter spherical test mass housed inside a 50 mm cubic cavity. The sphere’s position is sensed with a LED-based differential optical shadow sensor, its electric charge is controlled by photoemission using UV LEDs, and the spacecraft position is maintained with respect to the sphere using a cold gas micro-propulsion system. This paper highlights the history, applications, design, and laboratory technology development for this proposed CubeSat mission.

### INTRODUCTION

Next generation drag-free space systems<sup>1,2</sup> will provide autonomous precision orbit determination, more accurately map the static and time varying components of Earth’s mass distribution, aid in our understanding of the fundamental force of gravity, and ultimately open up a new window to our universe through the detection and observation of gravitational waves. At the heart of this technology is a gravitational reference sensor, which (a) contains and shields a free-floating test mass from all non-gravitational forces, and (b) precisely measures the position of the test mass inside the sensor. A feedback control system commands thrusters to fly the “tender” spacecraft with respect to the test mass. Thus, both test mass and spacecraft follow a pure geodesic in spacetime. By tracking the position of a low Earth orbiting drag-free satellite we can directly determine the detailed shape of geodesics and through

analysis, the higher order harmonics of the Earth’s geopotential. In addition to geodesic information, the commanded thrust, test mass position and GPS tracking data can be combined to produce 3 dimensional maps of atmospheric winds and density. With multiple drag-free spacecraft, one can perform a more accurate differential measurement between two geodesics, for example with laser interferometry, in order to improve measurements made by NASA’s twin GRACE satellites<sup>3</sup>.

The range of applications for drag-free technology is broad. A summary is provided in Table 1. The listed applications are separated into four distinct categories: navigation, Earth science, fundamental physics, and astrophysics. Two key performance metrics for each application are also shown. The first metric, called drag-free performance, is the residual acceleration of

the test mass in units of  $\text{m/sec}^2\text{Hz}^{1/2}$ . For an ideal drag-free satellite, the residual acceleration is zero, but in practice small, residual forces act on the test mass, perturbing its trajectory with respect to a pure geodesic. The primary goal of drag-free satellite design is to minimize these residual forces. The second metric, called metrology in Table 1, is either the measurement of the absolute position of a drag-free test mass (e.g. via GPS) or the differential measurement of the distance between two drag-free test masses.

**Table 1: Applications of Drag-free Technology**

Category	Application	Drag-free Performance ( $\text{m/sec}^2\text{Hz}^{1/2}$ ), frequency (Hz)	Metrology (m)
Navigation	Autonomous, fuel efficient orbit maintenance	$\leq 10^{-10}$ , near zero frequency <sup>a,b</sup>	$\leq 10$ absolute
	Precision real-time on-board navigation	$\leq 10^{-10}$ , near zero frequency <sup>a</sup>	$\leq 10$ absolute <sup>a</sup>
Earth science	Aeronomy	$\leq 10^{-10}$ , $10^{-2}$ to 1 Hz <sup>a</sup>	1 absolute <sup>a</sup>
	Geodesy, GRACE <sup>3</sup>	$10^{-10}$ , $10^{-2}$ to 1 Hz <sup>a,b,c</sup>	$10^{-6}$ differential <sup>a</sup>
	Future Earth geodesy <sup>4</sup>	$\leq 10^{-12}$ , $10^{-2}$ to 1 Hz <sup>a</sup>	$\leq 10^{-9}$ differential <sup>a</sup>
Fundamental physics	Equivalence Principle tests <sup>5</sup>	$\leq 10^{-10}$ , $10^{-2}$ to 1 Hz <sup>a</sup>	$\leq 10^{-10}$ differential <sup>a</sup>
	Tests of general relativity	$\leq 10^{-10}$ , near zero frequency <sup>a</sup>	$\leq 1$ absolute <sup>a</sup>
Astrophysics	Gravitational waves <sup>6</sup>	$3 \times 10^{-15}$ , $10^{-4}$ to 1 Hz	$\leq 10^{-11}$ differential

Notes: <sup>a</sup> Performance to be demonstrated by the drag-free CubeSat; <sup>b</sup> demonstrated; <sup>c</sup> non-drag-free

The first drag-free satellite, Triad I with the DISturbance Compensation System (DISCOS), launched in 1972, achieved a drag-free performance of better than  $10^{-10} \text{ m/sec}^2$  over 10-day periods and extended the time required for ephemeris updates to several weeks. Since then two other drag-free satellites have flown: NASA's Gravity Probe B (GP-B), which tested two predictions of general relativity with ultra-precise drag-free gyroscopes in low Earth orbit<sup>7</sup>, and ESA's geodesy mission, the Gravity field and steady-state Ocean Circulation Explorer (GOCE)<sup>8</sup>.

The measurement of Earth's gravity field is among the main goals of the NASA Earth Science program, as demonstrated by the GRACE mission. At the core of this mission are precision accelerometers that measure

all non-gravitational forces, which are removed from the gravitational measurements in the data post-processing. A drag-free system simplifies the data analysis by canceling the non-gravitational forces on-orbit and also allows for improved performance by reducing the dynamic range of the measurement.

In addition to Geodesy, drag-free technology enables precision distributed Earth-observing sensors, gravitational science and astrophysics missions, and precise orbit determination and maintenance. In a NASA Earth Science Technology Office Study on drag-free technology<sup>9</sup>, drag-free systems were found to have the following benefits: (a) a 50% reduction in fuel consumption for a continuously drag-compensated system compared with one corrected once after 4 weeks for a 350 km altitude satellite, (b) a 30%-50% reduction in navigation error if drag were directly compensated, and (c) a potential for substantial cost savings for drag-free satellite constellations in an orbit with substantial drag.

The target performance of the Drag-free CubeSat is  $10^{-11} \text{ m/sec}^2\text{Hz}^{1/2}$  between 10 mHz and 1 Hz, which is roughly 10 times better than the GRACE accelerometers and comparable to the drag-free performance of GOCE. The performance is limited primarily by the minimum impulse bit and thrust noise of available CubeSat scale thrusters. A propulsion system specifically tuned for a drag-free nano-satellite, would improve the performance by a factor of 10. After propulsion, the next largest disturbance forces are a function of the stability of the thermal and magnetic environment achievable on a CubeSat. All of the dominant error sources will be calibrated to  $10^{-12} \text{ m/sec}^2\text{Hz}^{1/2}$  through a series of plan on-orbit experiments.

The Modular Gravitational Reference Sensor (MGRS) utilizing a spherical test mass (TM) has been under development at Stanford for a wide range of applications since 2004<sup>10</sup>. The primary components of the MGRS, include a spherical TM, a LED based differential optical shadow sensor system for drag-free control, a caging (launch lock) mechanism based on the flight-proven DISCOS design<sup>14</sup>, and a charge control system based on the GP-B design but using modern LEDs as UV sources.

Magnetic, stray electric (patch effect), and other unwanted test mass forces depend strongly on and thus limited by, the gap between the TM which follows the geodesic and the test mass housing that encloses it and shields it from disturbances. Depending on the application, present gaps vary between fractions of a mm to a few mm, and can therefore be measured with

capacitance bridges. A spherical test mass requires no forcing or orientation control, and therefore does not require electrostatic suspension and allows for larger TM-to-housing gaps. In addition, optical measurements are superior in performance and simplicity, while requiring lower mass and power when compared with capacitive sensing.

The primary payload for the drag-free CubeSat will be scaled down version of the MGRS, developed at Stanford, which drives a cold gas thruster to compensate for drag and maintain the position of the satellite with respect to the test mass. The nominal propulsion system is a Micro-propulsion System (MiPS) produced by VACCO Space Products. The MiPS was chosen because it provides the best drag-free performance among the few flight ready micro-propulsion available. In the future, lower noise, lower minimum impulse bit thrusters could be used to improve the drag-free performance.

A commercial attitude control system will keep the satellite pointed in the direction of the drag force and control the satellite's roll angle. A commercial GPS system will be used to track the orbit.

## MISSION OVERVIEW

The Drag-free CubeSat is a 3-unit (3U) CubeSat, measuring 34 cm  $\times$  10 cm  $\times$  10 cm and weighing 4 kg at launch. The primary payload is a gravitational reference sensor, which consists of a cubical housing that contains and shields a free-floating spherical test mass. A differential optical shadow sensor (DOSS) mounted to four sides of the housing measures the position of the spacecraft with respect to the test mass in all 3 directions. The test mass, housing and associated electronics fill a volume equivalent to 1 unit of a CubeSat. Therefore we refer to this part of the payload as the 1U GRS. In addition, a caging mechanism is used to mechanically secure the test mass during launch and release it once the satellite reaches its designated orbit.

The drag-free control system uses the satellite position measurement provided by the shadow sensor and a small cold gas thruster in the aft of the satellite to compensate for atmospheric drag and keep the spacecraft centered with respect to the test mass. A commercially available Attitude Determination and Control System (ADACS) will maintain the satellite's attitude pointed in the direction of the drag force, as well as control the satellite's roll angle.

The primary science data consists of the DOSS position measurement, the commanded thrust, and the on-board GPS data. The 1U GRS is used to calibrate accurately

and continuously the thrust force. Therefore, the DOSS data plus the commanded thrust together provide a measurement of the external disturbing force, of which the atmospheric drag on the satellite is the largest. With the addition of attitude data, the drag force in 3 directions can be determined as well as any drag torques on the satellite. Full six-degree-of-freedom drag forces and torques will be estimated on the ground with frequencies up to 0.5 Hz.

GPS data will tie the drag information to orbital location, as well as provide the primary performance measurement. Estimates of the residual zero frequency non-gravitational acceleration acting on the satellite will be determined by fitting a model that includes the Earth's gravity field (e.g. GRACE Gravity Model 3), the DOSS position information, and the commanded thrust to the satellite GPS measurements. The residual zero frequency acceleration (in 3 directions) can be determined with an accuracy on the order of  $10^{-12}$  m/sec<sup>2</sup> from five days worth of drag-free flight data.

A detailed error budget, which includes 30 individual error sources has been compiled. The total residual acceleration of the test mass will be less than  $10^{-11}$  m/sec<sup>2</sup>Hz<sup>1/2</sup> and calibrated to better than  $10^{-12}$  m/sec<sup>2</sup>Hz<sup>1/2</sup>. The largest error terms will be bounded by three on-orbit tests:

1. Changing the spacecraft temperature with a heater mounted to the satellite structure,
2. Modulating an electro-magnetic source within the satellite, and
3. Systematically altering the center position of the satellite with respect to the test mass.

The largest error sources will be bounded, using mechanical, thermal and magnetic models of the Drag-free CubeSat and the on-orbit performance determined during these three tests.

## SATELLITE COMPONENTS AND LAYOUT

Figure 1 shows the layout of the drag-free CubeSat. The satellite is a standard 3U CubeSat. The main components are (a) a VACCO MiPS cold gas thruster in the aft end (-y), (b) the 1U GRS in the center unit with the a test mass at the satellite center of mass, (c) a test mass caging system to the aft of the 1U GRS, (d) spacecraft bus forward of the 1U GRS (+y) consisting of a motherboard, CPU, radio, and Electric Power System (EPS), and (e) the ADACS at the front of the satellite. The satellite structure is a custom designed aluminum frame.

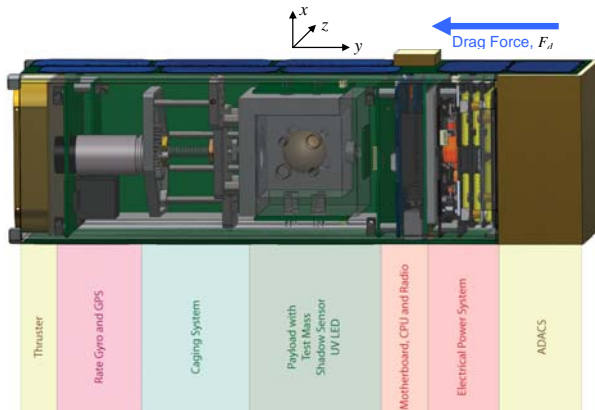


**Figure 1: CAD model of the Drag-free CubeSat**

### ***Payload Overview***

The payload consists of the test mass and housing, the DOSS position sensor, the UV LED charge control system, the caging mechanism, the cold gas thruster, the ADACS, and the drag-free control laws. The attitude and translation control system (thruster, ADACS and control laws) are considered part of the payload, since they are an integral part of the primary function of the satellite.

Figure 2 shows a cross section of the 1U GRS and caging mechanism. Both are mounted to a central titanium bulkhead which provides the only attachment point to the CubeSat structure. The bulkhead geometry and material are chosen to minimize the conductive heat path to the GRS housing. Thermal stability of the housing is important for the overall drag-free performance of the system. Each component is discussed separately below.

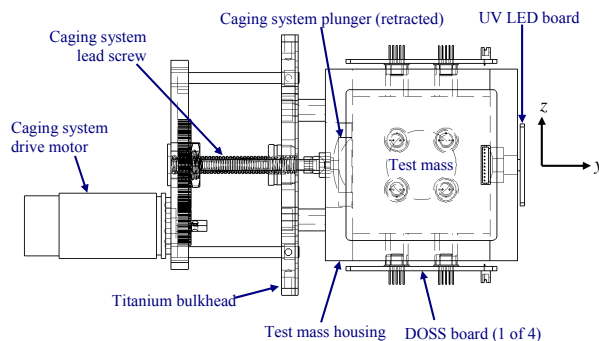


**Figure 2: Drawing of the 1U GRS (right), with caging mechanism (left). The large central plate is the titanium bulkhead**

### ***Test Mass and Housing***

The nominal test mass is a 25.4 mm (1 in.) diameter, 171 g sphere of 70%/30% Au/Pt. This material is chosen because it is dense, it can be machined, and it has a low magnetic susceptibility. The TM will be grade 10, i.e. round to 250 nm, which is a factor of 20× less round than the Gravity Probe B flight rotors<sup>11</sup>, and have a mass unbalance of < 1 μm, 100× that of the GP-B rotors. The TM and housing inner surface are coated in SiC, which has a quantum efficiency supporting UV charge control. In addition, SiC has a high elastic modulus and is extremely hard. Consequently, it is difficult to obtain large areas of contact, and therefore significant bonding with the spacecraft, even when constrained by a high preload<sup>12</sup>, for example during launch. The coatings of the TM and housing, which has no exposed sensitive components, are designed such that the TM can repeatedly touch the housing wall in a μg environment without damaging the TM or housing or sticking.

The housing is a 7 cm aluminum (6061-T6) cube with a 5 cm cubic internal cavity to accommodate the test mass. The housing is fabricated in two halves in order to allow its inner surface to be coated with SiC. Four faces (+x, -x, +z, -z) of the housing each have four holes to accommodate the emitters and detectors of the DOSS. The -y face of the housing has a 26 mm (1 inch) hole to accommodate the plunger of the caging mechanism, which, when actuated, holds the test mass against the +y inner face of the housing during launch. Recessed into the +y inner face of the housing is a UV LED used to control the electric charge on the test mass via UV photoemission. A sheet of mu-metal covers all external surfaces of the aluminum housing in order to magnetically shield the test mass. The magnetic shield is designed to reduce the magnetic field inside the house by a factor of 100 relative to the outside.

The 1U GRS mechanical design shown in Figure 2 is designed to attenuate thermal loads from the outside of the satellite. A COMSOL finite element model of the Drag-free CubeSat with the 1U GRS, ADACS, MiPS thruster, and additional mass to account for unmodeled components was created for both thermal and structural evaluation. A ±1 K sinusoidal temperature variation on the exterior surface of the satellite was applied as a boundary condition on the top (axial) and side (transverse) faces in separate analyses. Table 3 shows the axial and transverse thermal attenuation factors as a function of frequency. The attenuation factor represents the temperature difference on the interior surface of the housing at the specified frequency when a 1 K exterior temperature variation is applied at that same frequency. The drag-free performance budget discussed below uses

thermal attenuation factors that bound the values in Table 2.

**Table 2: Axial (z-axis) and transverse (x and y axes) thermal attenuation factor**

Frequency	1 mHz	10 mHz	100 mHz
Axial attenuation factor	$10^{-3}$	$10^{-5}$	$10^{-7}$
Transverse attenuation factor	$2 \times 10^{-3}$	$2 \times 10^{-5}$	$2 \times 10^{-7}$

The same FEA model was also used to perform a structural analysis of the Drag-free CubeSat. Based on the NASA General Environmental Verification Specification (GEVS), a bounding static load of 14.1 g was applied in the axial and transverse directions in separate analyses. The CubeSat and 1U GRS structure yield strengths are more than four time greater than bounding launch stresses.

### Differential Optical Shadow Sensor

The Differential Optical Shadow Sensor (DOSS) is the sensing system that measures the position of the test mass relative to the housing. This data is used as input to the drag-free and attitude control of the satellite. The DOSS is based on measuring light intensity thus allowing the use of non-coherent light sources. Its dynamic range is large and limited only by the size of the detector and the beam waist. Two light beams of equal intensity are tangent to and partially blocked by the TM. The two intensities and their difference are measured, thus canceling common mode noise in the signals. The measurement principle is illustrated in Figure 3 for a one dimensional measurement with one pair of detectors.

The DOSS requires two pairs of parallel beams for a three-dimensional position measurement. Four pairs are planned for redundancy. LEDs with a wavelength of 1550 nm are used for the light source. A low-power FET input amplifiers (such as the OPA129 or OPA140) is at the core of the amplifier. Data acquisition will use a DSP for lock-in detection and amplification.

A complete DOSS system has been developed and tested at Stanford, using flight like components and circuits (see Figure 4)<sup>13</sup>. Without using its differential capability the system has achieved a measured sensitivity of  $20 \text{ nm/Hz}^{1/2}$  above 10 mHz, with a  $1/f$  trend below 10 mHz. The noise amplitude spectral density is shown in Figure 5.

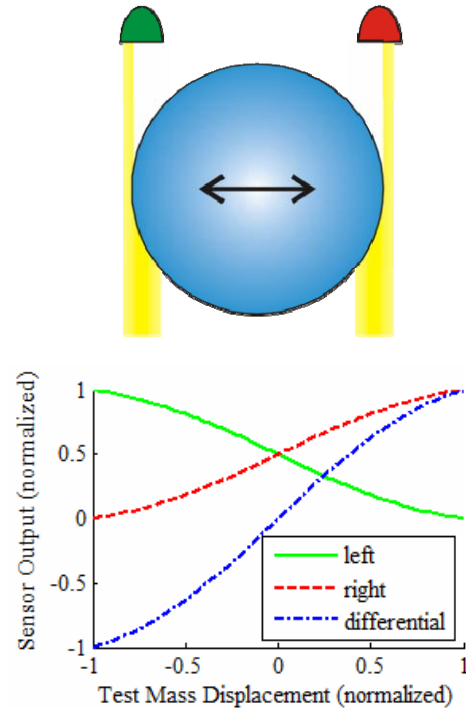


**Figure 3: Top: circular TM, two detectors and the partially blocked light beams. Bottom: simulation of the left and right signals and their difference**

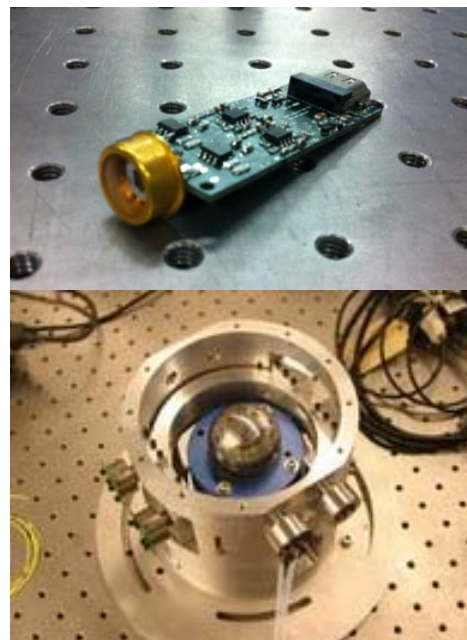


**Figure 4: Flight-like DOSS system. Photodetector (top): 3 mm FCI InGaAs quadrant photodiode with amplifier board containing power supply filter, first amplifier stage and 2nd stage differential amplifier. Bottom: complete system for a 50.8 mm sphere**

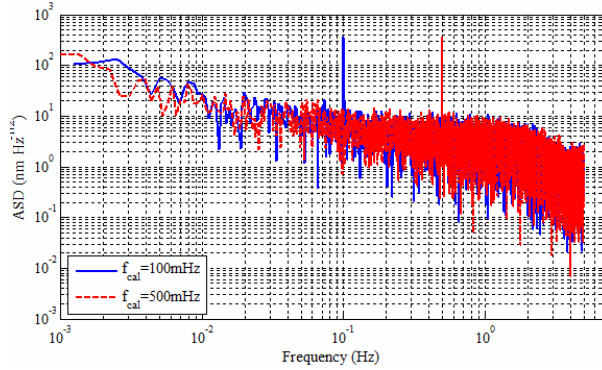


**Figure 5: Measured amplitude spectral density vs. frequency of the flight-like DOSS system at Stanford**

### ***Test Mass Caging Mechanism***

The fundamental requirements of the caging system are to prevent damage to the sphere during launch and to release the sphere after arrival of the satellite on orbit. The caging system and entire Drag-free CubeSat are designed to handle the prescribed NASA General Environmental Verification Specification (GEVS), which is 14.1 g-rms for the lightest satellites.

The caging system design, shown in Figure 6, is based on the flight-proven DISCOS system<sup>14</sup> and consists of a vacuum-compatible dc motor with gearbox, a moving “motor cart” to which said motor is mounted, a set of spur gears to transmit the output torque of the motor to a lead screw, a bronze nut into which the lead screw is threaded, a titanium bulkhead to which the nut is affixed, and which also acts as the attach point of the caging system to the spacecraft structure, a plunger on the end of the lead screw (the aforementioned actuated surface), and a set of precision-machined steel shafts and dry shaft bearings that guide the motion of the plunger. As designed, the total travel of the plunger is 25 mm, and the mass is 0.354 kg, including 0.120 kg for the motor.

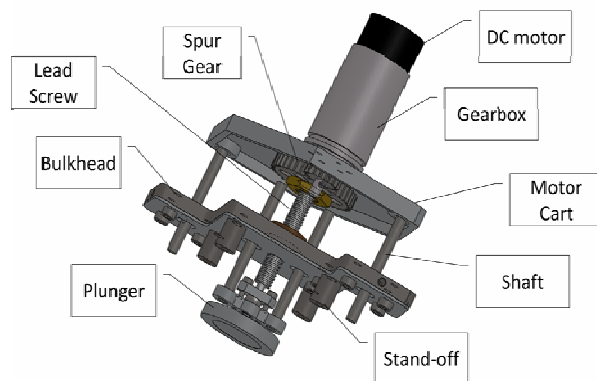


**Figure 6: Model of the test mass caging system**

To hedge against the possibility of binding after the plunger is engaged to the proof mass, the motor will be operated at two different voltages, so that the stall torque of the motor is higher when retracting the plunger than when engaging it. Although the ACME screw should prevent back-driving under most conditions, random vibration testing is planned to verify the pre-load remains at or above the required load of 200 N while the caging system is unpowered.

The measured magnetic flux density of the motor is 0.4 mT. Assuming a dipole approximation for the far field, the magnetic field strength at the nominal position of the proof mass (120 mm away, perpendicular to the dipole) would be 0.12  $\mu$ T, or less than 1/100th the strength of the Earth’s magnetic field at sea level.

### ***Test Mass Charge Control***

Charge management by UV photoemission using the 254 nm line of an rf mercury source was successfully demonstrated by the GP-B mission in 2004-2005. Newer technology allows the use of commercially available LEDs operating in the 240-255 nm range<sup>15</sup> as the UV source. Passive charge management will be used, relying on a virtual “wire” generated by photoemission and without bias is utilized for the proposed low capacitance 1U GRS. The power and mass are estimated at 0.1 W and 3 g, respectively. A number of UV-LED models have successfully completed environmental testing<sup>16</sup>, and a complete test mass charge control system<sup>17</sup> using UV LEDs will be demonstrated on a microsatellite in 2013.

### ***Micro-propulsion System***

The baseline propulsion system for the Drag-free CubeSat is the Micro-propulsion System (MiPS) produced by VACCO Space Products, shown in Figure 7. The drag-free CubeSat requires one thruster at the aft end in order to compensate for atmospheric drag. Each unit is 509 g, has a maximum thrust of 55 mN, specific impulse of 65 sec, and total impulse of 34 N-sec.

Thruster lifetime during drag-free operations as a function of the average orbit altitude is shown in Figure 8. The drag-free and attitude control system design discussed below assumes an average altitude of 400 km, resulting in a thruster lifetime of roughly 70 days. For comparison, the twin GRACE satellites fly at an altitude of roughly 450 km.

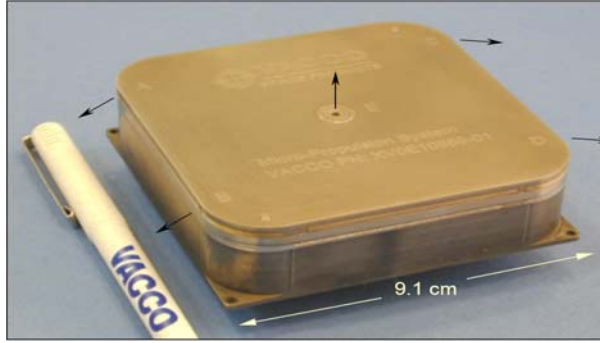


**Figure 7: VACCO Micro Propulsion System (Courtesy of VACCO Space Products)**

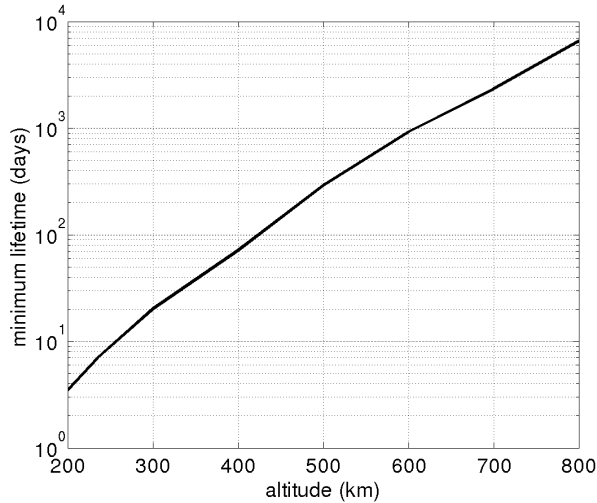


**Figure 8: Estimated lifetime of drag-free operation**

### *Drag-free and Attitude Control System*

The drag-free and attitude control system (DFACS) is a 6 degree-of-freedom (DOF) sensing and 4 DOF actuation system. The DFACS block diagram is shown in Figure 9. Drag-free (translation) actuation is performed with a single port of the MiPS thruster oriented in the  $-y$  direction, which opposes the main drag force. Attitude actuation is done with the Attitude Determination and Control System (ADACS) (baseline unit is the Maryland Aerospace MAI-400) at the front end ( $+y$ ) of the satellite. The primary 3 DOF translation sensor is the DOSS, with the IMU accelerometers (baseline unit is the Analog Devices ADIS16405) providing back-up information. Attitude sensing is a fusion of the horizon sensor that is part of the ADACS and the rate gyros included in the IMU. Both drag-free and attitude control inputs, as well as the output of both attitude and translation sensors are optimally combined by an Extended Kalman Filter (EKF), providing real-time attitude and translation estimates and covariances.

The transverse ports of the MiPS periodically desaturate the reaction wheels.

The control law design consists of relatively fast inner attitude control loop with a bandwidth of roughly 0.5 Hz and a slower drag-free outer control loop, operating at  $\sim 0.1$  Hz. Attitude and rate estimates (3 DOF), denoted  $\hat{\phi}$  and  $\hat{\omega}$  respectively, provided by the EKF are fed into the inner loop attitude controller, which sends a command,  $\mathbf{w}$ , to the reaction wheels of the ADACS. The reaction wheels provide the commanded torque,  $\mathbf{T}$ , to the spacecraft, which is also disturbed by atmospheric drag torques,  $\mathbf{D}$ .

The outer drag-free translation control is on/off with a single sided deadband, denoted DB. The size of the deadband depends on the minimum thrust bit and the drag force and therefore the nominal satellite altitude. Satellite position and velocity estimates in the  $y$ -direction,  $\hat{y}$  and  $\hat{v}$  respectively are fed to the on/off controller. When  $\hat{y} + \tau \hat{v}$  exceeds a threshold, the thruster is turned on. The parameter  $\tau$  defines the slope of this “switching line”. Taking the test mass as the reference position, the resulting motion of the spacecraft along the  $y$ -axis consists of parabolic arcs when plotted as  $y$  position versus time. Drag-free control in the transverse  $x$  and  $z$  directions is performed by adjusting the attitude to point the satellite in the direction opposite to the drag force.

A nonlinear numerical simulation of the DFACS has been implemented. It incorporates the satellite mass properties, the MiPS thruster performance, the DOSS and ADACS sensing noise, an ADACS torque limit of 10 mN-m, and simulated drag forces and torques for a 400 km circular polar orbit. The atmospheric drag model bounds the model used to design the GOCE drag-free control system<sup>8</sup>.

The resulting stable position and attitude (pitch and yaw only) of the Drag-free CubeSat are shown in Figure 10. The position origin is the center of mass of the test mass. The parabolic arcs,  $\sim 400 \mu\text{m}$  in amplitude, associated with the along-track satellite position are evident (blue curve). The transverse position of the satellite is maintained to within  $\pm 200 \mu\text{m}$ , and the pitch and yaw angles are  $< 10$  deg.

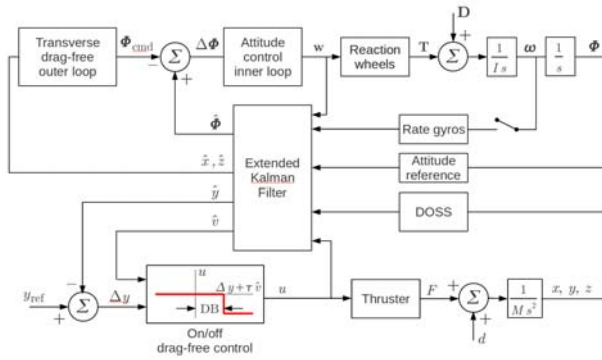


**Figure 9: Drag-free and attitude control system block diagram**

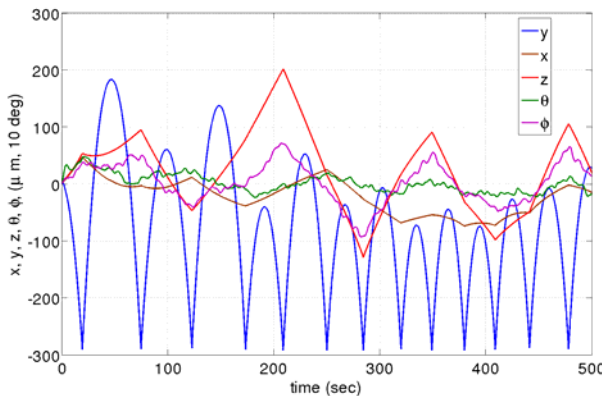


**Figure 10: Simulated performance of the Drag-free and attitude control system. Note:  $x, y, z$  position in units of  $\mu\text{m}$  and pitch angle,  $\theta$ , and yaw angle,  $\phi$  in units of 10 deg**

### Spacecraft

The spacecraft is a commercial 3U CubeSat bus such as the Pumpkin CubeSatKit with commercial EPS, ADACS, and GPS unit: payload volume  $10\text{ cm} \times 10\text{ cm} \times 26\text{ cm}$ . The electric power system (EPS) is powered by three solar panels, with 8 cells on each ( $\pm z$ , orbit normal sides and  $+x$ , radial, see Figure 1). When in sunlight, the power produced is 6.5-9.3 W, depending on the attitude. Batteries provide 30 W-h of power. This is sufficient to power all subsystems during drag-free operations with margin. If a Sun-synchronous orbit is not available, then drag-free operations must be intermittent or deployable solar arrays must be used.

Daily downlink is about 17 MB during drag-free operations, less when the satellite is not operated drag-free. The duration of drag-free operations is  $\sim 70$  days, assuming a 400 km average altitude. A commercial modem, transmitting and receiving over amateur radio frequencies is used to send telemetry and receive commands. Flash memory on board the satellite will be

sufficient to store all payload and spacecraft data for the entire mission. One GB of storage provides sufficient space to store about 1 year of operations data.

### EXPECTED PERFORMANCE

A detailed acceleration noise budget (drag-free performance) has been compiled for the Drag-free CubeSat. The budget contains 30 terms: 6 S/C-to-TM stiffness, 8 magnetic, 6 thermal, 4 electric, 4 Brownian, 1 cosmic ray, and 1 sensing noise term. Calculation of each term in the acceleration noise budget follows the methodology used for the Laser Interferometer Space Antenna (LISA) gravity wave mission<sup>18</sup>. The resulting composite acceleration noise and the 10 largest individual noise terms are shown as amplitude spectral densities in Figure 11. The dominant acceleration noise contribution is due to stiffness, which is the residual coupling (weak spring) between the satellite and test mass. The stiffness ( $\sim 10^{-6}\text{ m/sec}^2\text{m}$ ) is a composite of both gravitational and electromagnetic terms. The spectrum of the simulated motion of the satellite, shown in Figure 10, is multiplied by the stiffness to produce the associated acceleration noise. This noise term alone is  $\sim 10^{-11}\text{ m/sec}^2\text{Hz}^{1/2}$ . In order to estimate the acceleration noise to better than  $10^{-12}\text{ m/sec}^2\text{Hz}^{1/2}$  the stiffness contribution must be calibrated to at least 10%. The dashed curve in Figure 11 shows the uncalibrated performance and the solid black curve is the 10% calibrated performance. The calibration approach is discussed below

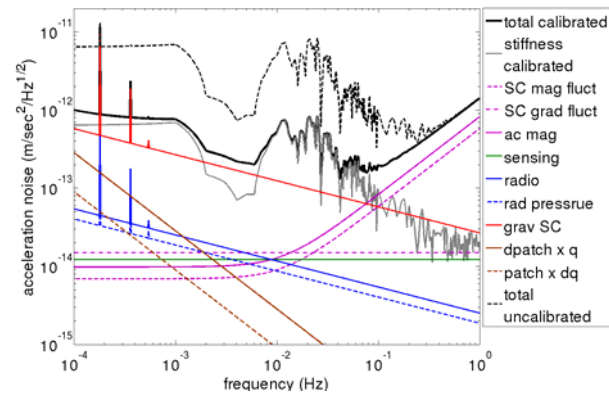


**Figure 11: Acceleration noise performance at an altitude of 400 km. The dashed and heavy black curves are the un-calibrated and calibrated composite acceleration noises respectively. The leading noise terms are: calibrated TM-to-satellite stiffness coupling to satellite motion (grey), self gravitation to the satellite (red), magnetic (magenta), electric disturbances (brown), thermal effects (blue), and optical sensing (green)**

The other two dominant error sources are magnetic interactions with the test mass (magenta curves in Figure 11), primarily above 100 mHz, and self-gravitation (red curve in Figure 11). Self-gravitation is the gravitational attraction of the TM to the satellite, which can be compensated for at low frequencies by carefully choosing the “zero” position of the satellite with respect to the test mass. At higher frequencies (as shown in Fig. 11) self-gravitation disturbances are driven by temperature changes, which change the geometry of the satellite via its coefficient of thermal expansion. The peaks in the self-gravitation and thermal terms are caused by temperature variations at harmonics of the orbit frequency. The three largest acceleration noise terms (stiffness, magnetic, and thermally driven self-gravitation) will be individually estimated by dedicated on-orbit tests.

### MISSION PROFILE

Launch is assumed to be as a secondary payload in compliance with the Poly Picosatellite Orbital Deployer (P-POD) launcher, accommodating 10×10×34 cm, into low earth orbit. A sun-sync orbit is preferred due to its constant solar illumination. The performance shown in Figure 10 assumes spacecraft thermal variations of  $\pm 20^\circ\text{C}$  variations at orbit, and  $\pm 1^\circ\text{C}$  at higher frequencies.

The Drag-free CubeSat flight is divided up into three mission phases: (a) launch and initial orbit checkout, (b) drag-free operations, and (c) post-drag-free operations. The total mission lifetime is limited by the amount of fuel contained in the MiPS thruster. Assuming an average altitude of 400 km, the total drag-free duration is  $\sim 70$  days depending on the on-orbit efficiency of the drag-free and attitude control system. Higher altitudes result in longer lifetimes, as shown in Figure 8.

During the initial orbit checkout, the test mass is caged and the thruster is kept off. The communications, EPS, UV LED charge control, DOSS, GPS, and DFACS (horizon sensor, rate gyros, magnetometers, reaction wheels) subsystems are all checked for proper functionality. Then, the attitude control system is used to establish nadir-fixed orientation control ( $y$ -axis is ram,  $z$ -axis is orbit normal,  $x$ -axis is radial pointing). Finally, the caging system releases the test mass and the DOSS is used to determine transient test mass dynamics and the final location of test mass inside housing.

At the start of the drag-free operations phase, the DFACS is activated and the test mass is “captured” by the satellite. The satellite is operated in a nominal drag-free mode for roughly 5 days. After this period of time, orbit estimation software on the ground is used to

estimate the low frequency acceleration bias (3-axis) of the satellite. Then the “center” position of the spacecraft with respect to the test mass is adjusted in order to compensate for the estimated acceleration bias. Drag-free operations are continued for another five days and a new acceleration bias estimate is produced and compensated for by re-centering the test mass sensor null. This process is repeated several times until a minimum zero-frequency acceleration bias is achieved.

Once the optimal drag-free performance is achieved, three test mass disturbance evaluation tests are performed. The first test involves modulating test mass center position at 1 mHz and using the DOSS and thrust profile to estimate the test mass-to-spacecraft stiffness. The second and third tests cycle heaters and electromagnets on board the spacecraft respectively with a 1000 sec periodicity in order to estimate the dependence of drag-free performance on temperature and magnetic field. After these three tests are completed nominal drag-free operations are resumed until all of the fuel is consumed.

During post-drag-free operations, the test mass is re-caged and un-caged several times and the DOSS is used to estimate test mass release dynamics. At the end of the mission, the test mass is re-caged and the satellite is shut down.

### DATA REDUCTION

The science data includes the vehicle time (clock), DOSS position measurement, commanded thrust, GPS data, attitude and torque commands, and environmental monitors (temperature, magnetic field, and UV LED drive signal). To reduce the data volume, the GPS data is a 3-dimensional position difference from a stored nominal orbit. From these data two science results are produced:

1. Atmospheric drag forces and torques, both as a time series and as a function of orbital position, and
2. Drag-free performance estimates, both at low frequency based on orbit estimation and at 1000 sec when intentionally driven by environmental factors (temperature, magnetic field, and spacecraft position).

The DOSS data plus the commanded thrust together provide a measurement of the atmospheric drag acting on the satellite in the ram ( $-y$ ) direction. The drag force in the 2 transverse directions ( $x$  and  $z$ ), as well as drag torques, will be estimated using the satellite’s attitude and applied torque.

Estimates of the residual zero-frequency non-gravitational acceleration acting on the satellite will be determined by fitting a model that includes the Earth's gravity field (e.g. GRACE Gravity Model 3), the DOSS position information, and the commanded thrust to the satellite GPS measurements. The residual zero-frequency acceleration (in 3 directions) can be determined with an accuracy of roughly  $10^{-12}$  m/sec<sup>2</sup> from five days worth of drag-free flight data. In addition the three largest individual sources of acceleration noise acting on the test mass will be bounded at a frequency of 1 mHz. This is done using mechanical, thermal and magnetic models of the Drag-free CubeSat and the on-orbit performance determined during three tests: 1) exciting the spacecraft temperature at 1 mHz with a heater mounted to the satellite structure, 2) modulating an electro-magnetic source within the satellite, and 3) systematically altering the center position of the satellite with respect to the test mass.

## CONCLUSION

The Drag-free CubeSat, a nano-satellite class drag-free mission, capable of state-of-the-art performance is proposed. The design is based on previous drag-free mission designs pioneered at Stanford University, but takes advantage of several new, low mass and low power component technologies. The design work performed to date demonstrates that an acceleration noise performance of  $10^{-11}$  m/sec<sup>2</sup>Hz<sup>1/2</sup> at 10 mHz is possible within the mass, volume, and power constraints of a 3U CubeSat.

Existing drag-free technology has been used for a specific class of medium to large science missions (>\$100M). The Drag-free CubeSat will transform our thinking of drag-free from an expensive, niche technology, to a low-cost, demonstrated solution to a wide range of applications. Constellations of autonomous drag-free small satellites for Earth observation, communications networks, Earth science, and fundamental physics would become possible.

## References

- DeBra, D.B. and J.W. Conklin, "Measurement of drag and its cancellation," *Classical and Quantum Gravity*, vol. 28, No. 9, May 2011.
- Buchman, S., R.L. Byer, J. Hanson, D.B. DeBra, D.L. Klinger, S.D. Williams, L.D. Dewell, D.B. Schaechter, N. Pedreiro, and D.J. Tenerelli. "Gravitational Reference Technologies: Critical for U.S. Space Leadership", a white paper, 2004.
- Tapley, B.D, S. Bettadpur, M. Watkins and C. Reigber, "The Gravity Recovery and Climate Experiment: Mission Overview and Early Results," *Geophys. Res. Lett.*, vol. 31, 2004.
- Barney, R.D. et al, "DRAFT Science Instruments, Observatories, and Sensor Systems Roadmap, Technology Area 08", NASA, November 2008.
- Touboul, P., M. Rodrigues, G. Metris and B. Tatry, "MICROSCOPE, testing the equivalence principle in space," *Comptes Rendus de l'Academie des Sciences Series IV Physics*, vol. 2, No. 9, November 2001.
- Danzmann K., and A. Rudiger, "LISA technology—concept, status, prospects", *Classical and Quantum Gravity*, vol. 20, 2003.
- Everitt, C.W.F. et al. "Gravity Probe B: Final Results of a Space Experiment to Test General Relativity," *Physical Review Letters*, vol. 106, No. 22, May 2011.
- Canuto, E., "Drag-free and attitude control for the GOCE satellite," *Automatica*, vol. 44, No. 7, July 2008.
- Leitner, J., "Investigation of Drag-Free Control Technology for Earth Science Constellation Missions," Final Study Report to NASA Earth Science Technology Office, 15 May 2003.
- Sun, K.-X., G. Allen, S. Buchman, R.L. Byer, J.W. Conklin, D.B. DeBra, D. Gill, A. Goh, S. Higuchi, P. Lu, N.A. Robertson and A.J. Swank, "Progress in Developing the Modular Gravitational Reference Sensor," *Proceedings of the Laser Interferometer Space Antenna: 6th International LISA Symposium, American Institute of Physics Conference Series*, vol. 873, November 2006.
- Keiser, G. M., "Gravity Probe B," *Proceedings of the International School of Physics "Enrico Fermi"*, *Atom Optics and Space Physics*, IOS Press, 2009.
- Bhushan, B., "Adhesion and stiction: Mechanisms, measurement techniques, and methods for reduction," *Journal of Vacuum Science & Technology B*, vol. 21, No. 6, 2003.
- Zoellner, A. et al, "Differential Optical Shadow Sensor (DOSS) Cubesat Payload," white paper in response to RFI Future Space Validation of Earth Science (NNH12ZDA005L), 2011.
- Hacker, R., J. Mathiesen and D.B. DeBra, "Caging Mechanism for a Drag-Free Satellite Position Sensor," *Proceedings of the JPL 10th Aerospace Mechanism Symposium*, April 1976.

15. Sun, K.-X., B.A. Allard, R.L. Byer and S. Buchman, "Charge management of electrically isolated objects via modulated photoelectric charge transfer," US patent US20080043397.
16. Balakrishnan, K., E. Hultgren, J. Goebel and K.-X. Sun, "Space Qualification Test Results of Deep UV LEDs for AC Charge Management," 11th Spacecraft Charging Technology Conference, poster presentation, September 2011.
17. Balakrishnan K. et al, "UV LED charge control of an electrically isolated proof mass in a Gravitational Reference Sensor configuration at 255 nm.," submitted to Classical and Quantum Gravity, preprint arXiv:1202.0585v1.
18. Gerardi, D., G. Allen, J.W. Conklin, K. Sun, D. DeBra, S. Buchman, P. Gath, W. Fichter, R.L. Byer and U. Johann, "Advanced drag-free concepts for future space-based interferometers: acceleration noise performance," arXiv:0910.0758, October 2009.